Wind tunnel blowing snow study: steady and unsteady properties of wind velocity, mass fluxes and mass exchanges

M. Naaim, F. Naaim-Bouvet, K. Nishimura, O. Abe, Y. Ito, M. Nemoto, K. Kosugi

M. Naaim, F. Naaim-Bouvet, K. Nishimura, O. Abe, Y. Ito, M. Nemoto, K. Kosugi. Wind tunnel blowing snow study: steady and unsteady properties of wind velocity, mass fluxes and mass exchanges. International Snow Science Workshop (ISSW 2013), Grenoble Chamonix-Mont-Blanc, France, October 7-11, 2013. pp. 114-119

WIND TUNNEL BLOWING SNOW STUDY: STEADY AND UNSTEADY PROPERTIES OF WIND VELOCITY, MASS FLUXES AND MASS EXCHANGES.

Mohamed Naaim[1,*], Florence NAAIM-BOUVET[1], Kouichi NISHIMURA[2], Osamu ABE[3], Yoichi ITO[2], Masaki NEMOTO[3], Kenji KOSUGI[3]

[1] Irstea, UR ETGR, Grenoble, France

[2] University of Nagoya, Japan

[3] Shinjo Branch, Snow and Ice Research Center (SIRC), National Research Institute for Earth Science and Disaster Prevention (NIED), Shinjo, Yamagata, Japan

ABSTRACT: Several CFD snow drift models were proposed in the literature. These models include various assumptions and scaling laws representing the mass exchange, the transport and diffusion of particles and the feedback on the air flow. The validations of such existing models were conducted over a partial set of data. This is one of the reasons why we carried out a series of experiments using the low temperature wind tunnel at Shinjo Branch of Snow and Ice Studies (CES : Cryospheric Environment Simulator), NIED in Shinjo, Yamagata Prefecture Japan. The first experiments we undertook allowed to characterize the used snow regarding the wind action. We placed an ultra-sonic anemometer and a snow particle counter at the end of the wind tunnel, and by increasing gradually the wind velocity until the snow entrainment start and we continued until attaining a significant snow fluxes and gradually decreasing the velocity until the transport vanished. We determined the threshold friction velocity. This procedure was conducted twice to evaluate the uncertainty of the determination. Secondly, and for three wind tunnel velocity (5.5 m/s, 7 m/s and 9 m/s) and using a snow depth sensor we measured the mass exchange rate at the base along the flow each 0.5 m and afterwards, we conducted the same experiments by measuring the basal wind velocity and mass fluxes each 1 m from the ground. Finally and at the end of the wind tunnel, where the steady state is clearly attained and using an ultrasonic anemometer and a snow particle counter, we explored the vertical velocity and mass flux evolution. These data are analyzed to explore the macroscopic scaling law relating the mass exchange to the air flow velocity and the mass fluxes and the relation between the horizontal mass flux and the mean velocity. Since these data cover a significant range of flow velocity and include the determination of grain characteristics, the threshold velocity, the erosion fluxes, the air flow and snow fluxes at the interface between the air and the snow at rest, along the flow in the unsteady phase and the vertical snow fluxes and wind velocity profiles in the steady phase, it is a good opportunity to use these data to conduct an international benchmark between available snow drift CFD numerical models.

KEYWORDS: Wind, boundary layer, snow, drifting snow, experimental investigations, saltation, roughness, erosion rate.

1. INTRODUCTION

Since, blowing snow may cause inconveniences, disturbances and obstacles to the human activities, intensive research, using wind tunnel (Sato 2001, Nemoto 2001, Okaze 2012) and *in situ* test studies (Takeuchi 1980, Pomeroy , Naaim-Bouvet et al. 2012) were conducted, during the last decades, to understand the physical processes involved and establish the relationships governing the initiation and the development of this geophysical phenomenon. Several numerical models (Sundbo et al. 1997, Naaim et al. 1998, Gauer 2001, Durand et al. 2004, Kok et al. 2009, …) were simultaneously, developed. These models use relevant coupling between the dynamics of the fluid and the snow particles. Among them, several solved the mass and momentum conservation equations for solid and fluid phases. To close the system of equations several empirical equations, accounting for erosion, for entrainment and for the feedback of the solid discharge on air flow, were used.

The objective of experimental studies reported in this paper, is to obtain a complete set of data required to intercompare existing models and analyze, the relevance of their assumptions.

Corresponding author address: Mohamed Naaim, UR ETGR, 2 Rue de la papeterie,
Domaine Universitaire, 38402, France
tel: +33 4 76 76 27 22 ;
email: mohamed.naaim@irstea.fr

M. Naaim, F. Naaim-Bouvet, K. Nishimura, O. Abe, Y. Ito, M. Nemoto, K. Kosugi. Wind tunnel blowing snow study: steady and unsteady properties of wind velocity, mass fluxes and mass exchanges. International Snow Science Workshop (ISSW 2013), Grenoble Chamonix-Mont-Blanc, France, October 7-11, 2013. pp. 114-119

2. WIND TUNNEL AND SNOW CHARACTERISTICS

The wind-tunnel, used in this study, is installed in a cold room in the Cryospheric Environment Simulator at the Shinjo Branch, Snow and Ice Research Center. The length of the test section is 14 m and its cross-sectional area is 1 m^2 (see Figure 2). The walls are made of glass plates and metallic frames. More details of the wind tunnel can be found in Sato et al. 2001 and Nemoto et al. 2001.

The following notation will be used. The longitudinal axis is noted Ox. It originates at the beginning of the loose snow. The first 0.5 m of the test section are systematically filled with a layer of hard snow of 2 cm height. Oz is the vertical axis. The transversal axis is noted Oy. In the Cartesian system of coordinates Oxyz, the wind velocity vector is noted $\vec{u} = (u, v, w)$.

During our experiments, the temperature of the wind tunnel was maintained at - 10°C. For each experiment, a loose snow, made according to a specific process of NIED, was sifted and spread out on the floor of the entire study section, forming a homogeneous snow bed layer of 2 cm thickness with a flat surface. The size of the particles obtained varies from 100 µm for grains to 1 mm for clusters of grains (see Figure 1). The density of the loose snow is about 370 $kg.m^{-3}$. Before the beginning of each run, the snow is removed and sieved to reduce its cohesion allowing to start all the experiments with the same loose snow. The duration of experiments, varied from 5 to 15 minutes. It was reduced to the minimum to avoid sintering.

The wind velocity at the input center section of the wind tunnel is the control parameter. All the other parameters, related to the geometry of the wind tunnel and to the snow, were maintained as constant as possible although the uncertainties inherent to measurements and to the variability of the snow properties must be kept in mind.

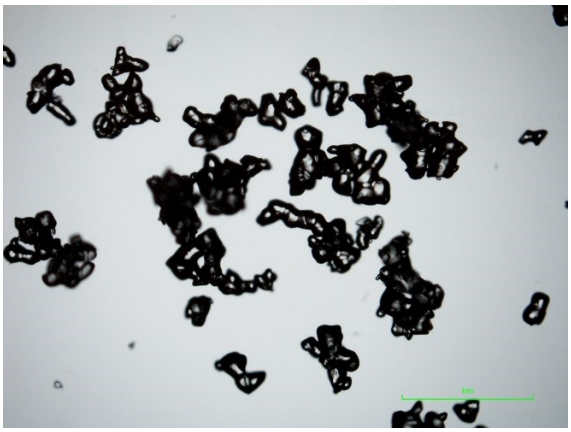

Figure 1. Photo of snow grains and clusters.

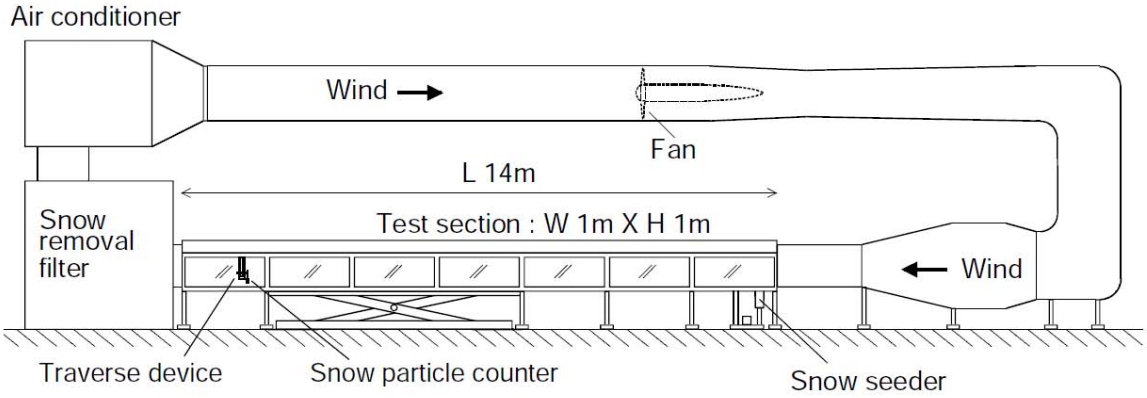

Figure 2: Schematic diagram of the wind tunnel (from Kosugi et al. 2008)

3. MEASUREMENTS TECHNIQUES

We used three different sensors in this experimental campaign:

- The first one is SPC (SPC-S7, Niigata Electric Co., Ltd.); an optical instrument allowing to measure the snow mass flux (see Sato et al 1993) (Figure 3).
- The second sensor in an ultrasonic anemometer that measures the three components of the wind velocity. The frequency bandwidth of this sensor is limited to 20 Hz (Figure 3).
- The third one is a Keyence distance meter, used here to measure the snow depth (Figure 4).

M. Naaim, F. Naaim-Bouvet, K. Nishimura, O. Abe, Y. Ito, M. Nemoto, K. Kosugi. Wind tunnel blowing snow study: steady and unsteady properties of wind velocity, mass fluxes and mass exchanges. International Snow Science Workshop (ISSW 2013), Grenoble Chamonix-Mont-Blanc, France, October 7-11, 2013. pp. 114-119

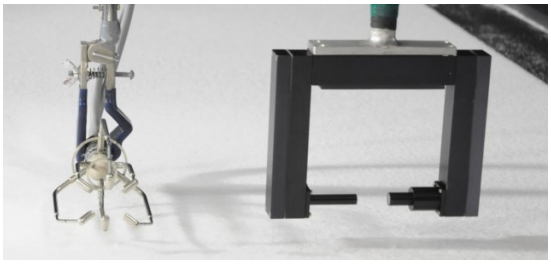

Figure 3. Ultra-sonic anemometer and SPC

Figure 4. The Keyence distance meter.

4. CONDUCTED EXPERIMENTS

In order to characterize the aerodynamic behavior of the wind tunnel and determine the relation between the mean speed, at the entrance (noted u_c), and the velocity profile characteristics at the end of the wind tunnel we conducted the following experiment. We fixed the wind tunnel speed at u_c=4.8 m.s^{-1}. Beyond this speed the snow erosion and entrainment occur.

The bottom of the wind tunnel is uniformly covered with loose snow. The wind velocity is measured, each 5 mm, from 0.03 m to 0.37 m, thanks to the ultrasonic sensor. The SPC is simultaneously used to check the absence of blowing snow. Due to the size of the anemometer; the lowest measurement point is 3 cm from the snow surface. The obtained profile is plotted on figure 6. To determine the turbulent friction velocity and the roughness length, we fit a logarithmic function on the measurements made between 3 cm and 10 cm since beyond 10 cm the profile shape change and becomes quasi linear.

$$u(z) = \frac{0.22}{k} ln\left[\frac{z}{110\ 10^{-4}}\right] \quad (1)$$

In equation (1) k, equal to 0.41 m.s^{-1}, is the van Karman constant. The obtained friction velocity is 0.22 m.s^{-1} and the roughness length, without blowing snow, is 110 10^{-6} m close to the snow grain size.

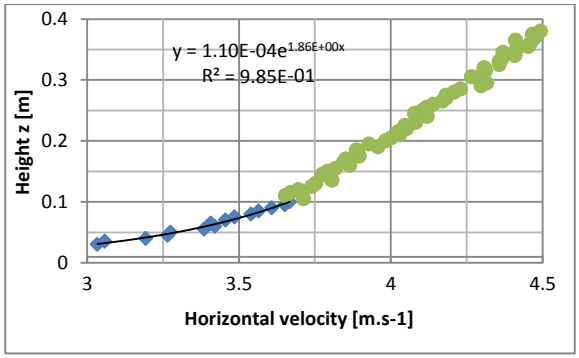

Figure 6: Velocity profile at the downstream end of the wind tunnel - in the absence of blowing snow.

Since the acquisition frequency of the ultrasonic anemometer has been is sat to 200 Hz and the measurement duration at each height was 30 seconds, 6000 measures are performed at each height and used to determine the mean velocity and the Reynolds turbulent friction velocity. As expected (bandwidth of sensor) , the spectrum of the velocity showed that beyond 20 Hz, the energy is 5 orders lower than in the range 0-10 Hz (see figure 5).

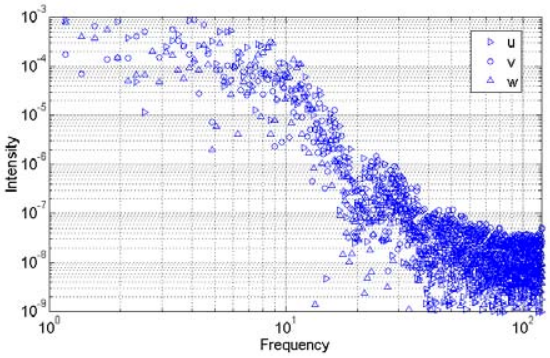

Figure 5. Spectrum of the velocity near the bottom at the downstream end the wind tunnel.

Despite the bandwidth, we calculated close to the bottom (3 cm) the Reynolds friction velocity using the standard formula 2:

$$u_* = \sqrt{\sum(u_i - \overline{u_i})(u_j - \overline{u_j})} \quad (2)$$

We obtained u_*=0.21 m.s^{-1}. This value is equal to the one determined by the logarithmic fit. Despite the bandwidth of the ultrasonic sensor, the two methods gave the same evaluation of the turbulent friction velocity.

The ratio of the friction velocity at the downstream end of the wind tunnel, to U_c, is 0.044. Since the flow is turbulent and rough, in the absence of blowing snow, this ratio will be considered constant whatever the entrance velocity.

The erosion of the snow mantle when submitted to the wind action is determined by the

M. Naaim, F. Naaim-Bouvet, K. Nishimura, O. Abe, Y. Ito, M. Nemoto, K. Kosugi. Wind tunnel blowing snow study: steady and unsteady properties of wind velocity, mass fluxes and mass exchanges. International Snow Science Workshop (ISSW 2013), Grenoble Chamonix-Mont-Blanc, France, October 7-11, 2013. pp. 114-119

threshold aerodynamic force, beyond which the transport starts and under which, the transport stops. It is generally determined through the corresponding turbulent friction velocity. To determine the threshold friction velocity corresponding to the used loose snow, we conducted, twice, the same experiment. A layer of snow is uniformly deposited over the whole wind tunnel. The snow particle counter is placed at the upstream end of the wind tunnel. The wind velocity is gradually increased, step by step, until the snow entrainment starts and attains a significant snow flux. Afterwards we gradually decreased the velocity until the transport vanished.

We plotted on Figures 6, the mass flow rate obtained function of the turbulent velocity determined by multiplying this latter by the coefficient 0.044 deduced from the above experiment. The values of the mass flux we used in these figures are averaged over 30 seconds. In the first experiment (figure 6, test 1, blue), during the ascending phase, the mass flow rate passes the threshold of 0.01 $kg.m^{-2}.s^{-1}$ for a turbulent friction velocity of 0.2 m. s^{-1}, whereas for the descending phase the transport flow rate falls below 0.01 $kg.m^{-2}.s^{-1}$ for a turbulent friction velocity of 0.21 m. s^{-1}. In the second experiment (figure 6, test 2, red), during the ascending phase, the mass flow rate passes the threshold of 0.01 $kg.m^{-2}.s^{-1}$ for a turbulent friction velocity 0.21 m. s^{-1}, and for the descending phase the mass flow rate falls below 0.01 $kg.m^{-2}.s^{-1}$ for a turbulent friction velocity of 0.21 m. s^{-1}. We therefore retained as threshold turbulent friction velocity u_{*t}= 0.21 m. s^{-1}.

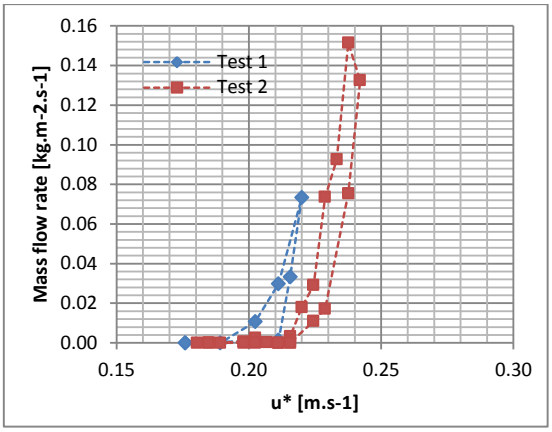

Figure 6: Mass flow rate at the downstream end of the wind tunnel function of the turbulent friction velocity.

In order to investigate the temporal and spatial evolution of the erosion, two types of experiments were conducted. For each of these experiments, loose snow is sifted and spread out homogeneously on the floor of the working section, forming a snow bed of 2 cm thick and the wind tunnel is run at fixed velocity (5.5 $m.s^{-1}$, 7 ms^{-1} and 9 ms^{-1}). In the first type of experiment, a longitudinal snow surface profile is performed before and after the experiment consisting in running the wind tunnel during a fixed lapse of time at a fixed velocity (4 minutes for 5.5 ms^{-1} and 7 ms^{-1} and 2 minutes for 9 ms^{-1}). The difference between the two profiles is performed and serves to determine the evolution of the erosion rate along the wind tunnel. The figure 7, for instance, shows the longitudinal distribution of the erosion rate obtained for U_c=7$m.s^{-1}$. The second type of experiment consisted in measuring simultaneously the mass flux at 1 cm and the wind velocity at 3 cm each 1m from 0.5 m to 11.5 m. The figure 8 shows, for instance, the longitudinal distribution of the mass flux as function of the longitudinal distance for U_c=7$m.s^{-1}$.

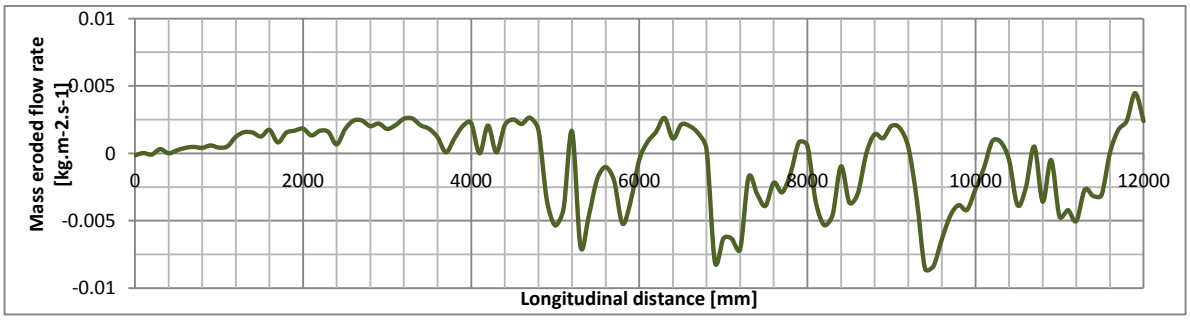

Figure 7: Longitudinal distribution of the mass erosion rate for U_c=7$m.s^{-1}$.

M. Naaim, F. Naaim-Bouvet, K. Nishimura, O. Abe, Y. Ito, M. Nemoto, K. Kosugi. Wind tunnel blowing snow study: steady and unsteady properties of wind velocity, mass fluxes and mass exchanges. International Snow Science Workshop (ISSW 2013), Grenoble Chamonix-Mont-Blanc, France, October 7-11, 2013. pp. 114-119

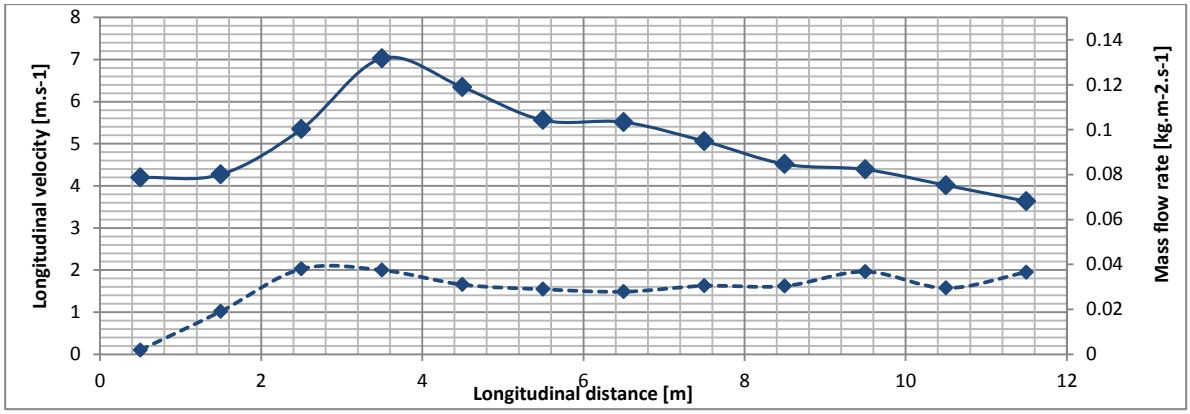

Figure 8: Longitudinal evolution of mass flow rate at z=1 cm and air flow velocity at z=3 cm for U_c=7m.s^{-1} (full line velocity and dashed line mass flux).

Among several other results, these data allowed drawing up the relationships linking the mean mass flux to (u_*-u_{*t}).The relation is a quasi linear function.

The terminal mass flux measured at 1 cm at the upstream end of the wind tunnel, is plotted in figure 9, function of the mean mass flux determined from the topography evolution. A very nice linear trend is shown indicating that 60% of the mass eroded is transported in the first centimetre where the saltation phenomenon dominates.

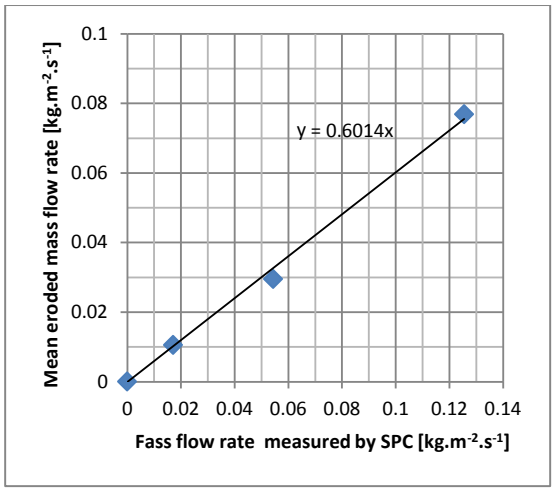

Figure 9: Mass erosion per unit area and per second deduced from the snow depth variation as a function of the mass flow rate measured at z=1 cm and x=11.5 m.

Finally, we investigated the vertical distribution of the velocity (figure 10) and the mass flux (figure 11) at the downstream end of the wind tunnel for the same three entering velocities. From these profiles we deduced the friction velocity, the roughness length and the depth average transported mass. These data are used to quantify the effect of the turbulent friction velocities on the roughness length and the total mass flux.

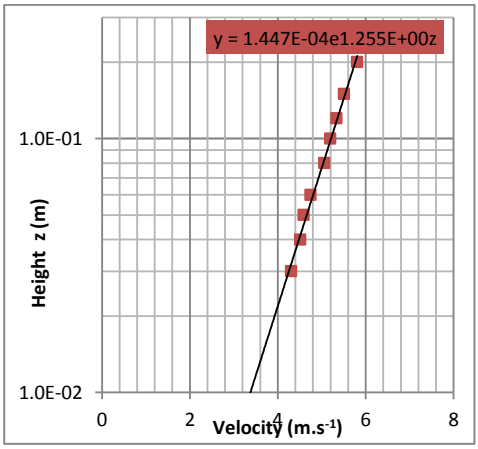

Figure 10: Velocity profile at x=11.5 m for U_c=7m.s^{-1}. The fits allow determining the turbulent friction velocity and the roughness length.

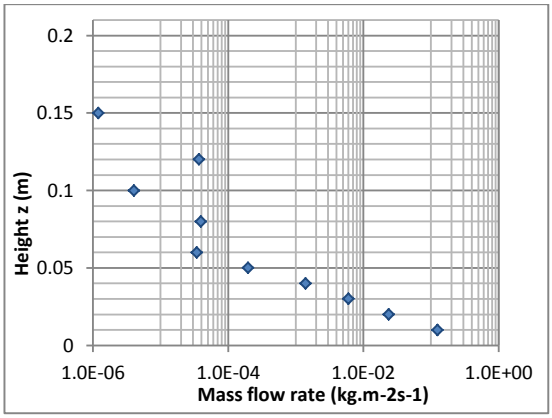

Figure 11: Mass fluxes, recorded by SPC at the centre of the wind tunnel at x=11.5 m, function of z for for U_c=7m.s^{-1}.

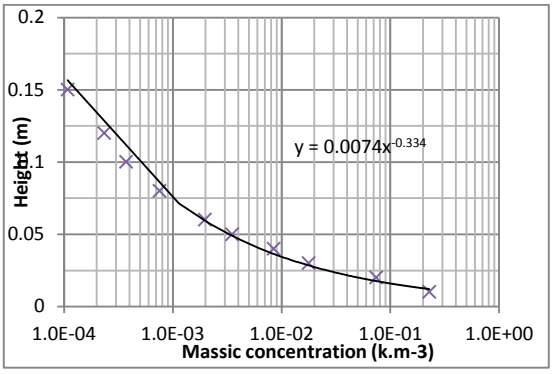

Figure 14: Massic concentration profile at x=11.5 m for for U_c=9m.s^{-1}.

5. OUTCOMES

Wind tunnel experiments, over loose snow surface, were carried out to investigate the characteristics of blowing snow phenomena. An experimental well-documented data base was therefore set up. The snow drift and its consequences in terms mass flux, feedbacks on air flow, vertical and horizontal structuration of the mass and the consequences on the topography modifications are measured for three different entering velocities, one which is close to threshold velocity. The snow is characterized by its density and hardness but also by its threshold turbulent friction velocity for which a specific test was devoted.

These data will be proposed for a common benchmarking of existing numerical models. In addition, the ongoing analyzes, are very promising. The scaling laws, relating the mass flux, the roughness length, the erosion rate, according to the turbulent friction velocity, the threshold turbulent friction velocity and the fall velocity, are very interesting. They will be submitted for publication in the coming months.

6. ACKNOWLEDGEMENT

The authors thank very warmly the NIED director for giving access to the exceptional simulator. The authors also want to thank T. Takeda and G. Okawa for operating the wind-tunnel and for their assistance during the entire week of experiments.

7. REFERENCES

Bang,B., Nielsen,A., Sundsbø, P.A., Wiik, T., 1994. Computer simulation of wind speed, wind pressure and snow accumulation around builings (SNOW SIM). Energy and Buildings 21, 235–243.

Bintanja, R., 2001. Modification of the wind speed profile caused by snowdrift: results from observations. Quarterly Journal of the Royal Meteorological Society 127, 2417–2434.

Durand, Y., Guyomarc'h, G., Rindol, L., et Corripio, J.:2004. Two-dimensional numerical modelling of surface wind velocity and associated snowdrift effects over complex mountainous topography, Ann. Glaciol., 38, 59–70.

Gauer, P., 2001, Numerical modeling of blowing and drifting snow in Alpine terrain, J. Glaciol., 47, 97-110.

Kok, J., Renno, N., 2009, A comprehensive numerical model of steady state saltation, J. Geophys. Res., 114, D17 204, 2009.

Kosugi, K., Sato, T., Nemoto, M. , Mochizuki, S., and Sato, A., 2008, Vertical profiles of mass flux for different particle diameters in drifting snow over hard snow surfaces, Proceeding of the ISSW 2008, Whistler, USA.

Michaux, J.L, Naaim-Bouvet, F. and M. Naaim. (2001). - Drifting-snow studies over an instrumented mountainous site : II. Measurements and numerical model at small scale. Annals of Glaciology, 32: 175-181.

Naaim, M., Naaim-Bouvet, F., et Martinez, H., 1998. Numerical simulation of drifting snow: erosion and deposition models, Ann. Glaciol., 26, 191-196.

Naaim-Bouvet, F., Naaim, M., Bellot, H. and K. Nishimura (2011). – Wind and drifting snow gust factor in an Alpine context. Annals of Glaciology, 58(52): 223-230.

Nemoto, M., Nishimura, K., 2001. Direct measurement of shear stress during snow saltation. Boundary-Layer Meteorology 100, 149–170.Pomeroy, J.W., Gray, D.M., 1990. Saltation of snow. Water Resources Research 26 (7), 1583–1594.

Okaze T., Mochida A., Tominaga, Y., Nemoto M., Sato, T. , Sasaki Y., Ichinohe, K., 2012, Wind tunnel investigation of drifting snow development in a boundary layer J.WindEng.Ind.Aerodyn.104–106(2012)532–539

Sato, T., Kimura, K., Ishimura, T., Maruyama, T., 1993. Field test of a new snow particle counter(SPC) system. Annals of Glaciology 18,149-154.

Sato, T., Kosugi, K., Sato, A., 2001. Saltation-layer structure of drifting snow observed in a wind tunnel. Ann. Glaciol. 32, 203-208.

Sato, T., Kosugi, K., Sato, A., 2004. Development of saltation layer of drifting snow. Ann. Glaciol. 38, 35-38.

Sundsbø, P. , 1997, Numerical modelling and simulation of snow drift, Ph.D. thesis, Ph. D. thesis, Norwegian University of Science and Technology, Trondheim.

Takeuchi, M., 1980. Vertical profiles and horizontal increase of drifting snow transport. Journal of Glaciology 26 (94), 481–492.